13th Australia New Zealand Conference on Geomechanics – Acosta-Martínez & Lehane (Eds.)

Application of the method of manufactured solutions in code verification in geomechanics

A. Khoshghalb & O. Ghaffaripour
UNSW Sydney, Sydney, Australia

K. Zamani
Wood Rodgers Inc., CA, USA

ABSTRACT: The paper presents the application of the method of manufactured solutions (MMS) as a verification tool for numerical codes in geomechanics. For this purpose, a coupled flow and deformation code for poro-elastic media developed using FORTRAN programming language based on the edge-based smoothed point interpolation method (ESPIM) is verified. In the ESPIM, the problem domain is spatially discretised using a triangular background mesh, and the smoothing domains are then formed on top of the background mesh. The polynomial point interpolation method (PIM) combined with a simple node selection scheme is adopted for creating nodal shape functions. Verification of the code is performed through an example in which independent manufactured solutions (MSs) for displacement and pore pressure fields are constructed as functions of both space and time. The solutions are then used to obtain the source terms of the governing equations, and boundary conditions. The problem is solved numerically followed by a thorough order of accuracy study. The steps required for a thorough code verification is detailed. The study shows that MMS is an excellent tool in verifying the code, and that the tested code passes the order of accuracy test successfully.

1 BACKGROUND

Different techniques are available for scientific code verification. The least reliable code verification approach is to seek an expert opinion on the outputs of a code (Roy, 2005). There are also some simple tests that can be performed to detect any potential problem with a code, such as the geometric symmetry test, and the conservation tests in which conservation of different variables such as mass and energy is evaluated according to the physics of the problem of interest (Oberkampf and Roy, 2010). Another common verification approach is code-to-code comparison which includes comparing the results of two codes with the same mathematical and physical basis.

These approaches are all useful, but cannot be used as a substitute for a rigorous verification assessment (Oberkampf and Roy, 2010). Discretisation error evaluation is another criterion in which the numerical results from a discrete model obtained from spatial and/or time discretisation are compared with an exact or benchmark solution (Oberkampf and Roy, 2010). This type of verification should always be accompanied with a discussion stating whether the discretisation error is small enough or not. Convergence test is the assessment of the rate in which the discretisation error is reduced as the mesh size decreases. A more comprehensive version of this verification test is the order of accuracy study. The order of accuracy study not only concerns studying the error reduction rate, but also compares this rate with the theoretical order of accuracy, often referred to as the formal order of accuracy.

This paper first presents a brief description of the differential equations governing the behaviour of saturated porous media. The numerical model of the problem is then developed through discretisation of the governing equations in space and time. Then a brief description of the method of manufactured solutions (MMS) and order of accuracy study is presented. Accordingly, an in-house fully coupled flow deformation code written based on a meshfree method called smoothed point interpolation method (SPIM) is verified to provide an example of the steps required for code verification for coupled problems in geomechanics using MMS.

2 GOVERNING EQUATIONS

According to the theory of mixtures, a saturated porous medium is assumed to comprise two continuous interacting continuum phases, solid skeleton (or solid matrix) and pore fluid. The general equations governing flow and deformation in a saturated deforming porous medium assuming an incompressible solid phase are expressed as follows (Lewis and Schrefler, 1999),

$$\partial^{\mathrm{T}}\boldsymbol{\sigma} + \mathbf{F} = \mathbf{0} \tag{1}$$

$$\mathrm{div}\left[\frac{\mathbf{k}}{\mu_{\mathrm{w}}}\left(\nabla p + \rho_{\mathrm{w}}\mathbf{g}\right)\right] = a_{\mathrm{w}}\dot{p} + \mathrm{div}(\dot{\mathbf{u}}) \tag{2}$$

where ∂ is the differentiation matrix, ∇ is the gradient operator matrix defined as $\nabla = \partial^{\mathrm{T}}\boldsymbol{\delta}$, with $\boldsymbol{\delta} = \begin{bmatrix}1 & 1 & 0\end{bmatrix}^{\mathrm{T}}$, and div stands for the divergence operator. In these equations, bold imprints denote

vectors and matrices. $\boldsymbol{\sigma}$ is the total stress vector with $\boldsymbol{\sigma}=\mathbf{D}\boldsymbol{\varepsilon}+p\boldsymbol{\delta}$, $\boldsymbol{\varepsilon}=\partial\mathbf{u}$ is the Cauchy small strain vector, $\mathbf{D}$ is the elastic stiffness matrix, p is the pore water pressure, $\mathbf{u}$ is the soil displacement vector, $\mathbf{F}$ is the vector of body force per unit volume, $\mathbf{g}$ is the gravity acceleration vector; $\mathbf{k}$ is the intrinsic permeability matrix, μ_{w} is the water dynamic viscosity, ρ_{f} is the water density, and $a_{\mathrm{w}}=nc_{\mathrm{w}}$, where n is the porosity and c_{w} is the water compressibility.

3 EDGE BASED SMOOTHED POINT INTERPOLATION METHOD

In the current study, the generalised smoothed Galerkin (GS-Galerkin) weakened weak formulation (Liu and Zhang, 2013) is employed to discretise the governing equations. For this purpose, smoothing domains are constructed on top of a triangular background mesh and a constant smoothed strain is assigned to each smoothing domain. Construction of the smoothing domains is performed based on the edges of the triangular background cells. A novel approach is adopted for taking the coupling effect of solid and fluid phases into account (Ghaffaripour et al., 2017). To secure non-singularity of the moment matrix, a simple node selection scheme is employed in which three nodes of the cell hosting the Gauss point of interest are selected as the supporting nodes, and the polynomial point interpolation method (PIM) (Liu and Gu, 2001) is considered for determination of the nodal shape functions for both fluid and solid phases.

Constant strains are assigned to each eadge-based smoothing domain which can be obtained from the following integration:

$$\bar{\boldsymbol{\varepsilon}}_k=\left(\int_{\Gamma_k^{\mathrm{SD}}}\mathbf{L}_{\mathrm{n}}\mathbf{u}(\mathbf{x})\mathrm{d}\Gamma\right)/A_k^{\mathrm{SD}} \tag{3}$$

where $\bar{\boldsymbol{\varepsilon}}_k$ is the constant smoothed strain over the kth smoothing domain with the boundary Γ_k^{SD}, A_k^{SD} is the area of the kth smoothing domain, and $\mathbf{L}_{\mathrm{n}}$ is the matrix of the unit outward normal vector.

4 SPATIAL AND TEMPORAL DISCRETISATION

The governing equations (1) and (2) are discretised adopting the GS-Galerkin method, as follows:

$$\mathbf{KU}+\mathbf{QP}=\mathbf{F}_{\mathrm{s}} \tag{4}$$

$$\mathbf{Q}^{\mathrm{T}}\dot{\mathbf{U}}-\mathbf{HP}-\bar{a}_{\mathrm{w}}\mathbf{S}\dot{\mathbf{P}}=\mathbf{F}_{\mathrm{w}} \tag{5}$$

where $\mathbf{U}$ is the vector of nodal displacements, $\mathbf{P}$ is the nodal pore fluid pressure vector, $\mathbf{F}_{\mathrm{s}}$ is the vector of nodal forces, $\mathbf{F}_{\mathrm{w}}$ is the vector of nodal fluxes, and $\mathbf{Q}$, $\mathbf{S}$ and $\mathbf{H}$ are the global property matrices of the system which are evaluated by assembling the local matrices obtained for each smoothing domain. For more details in this regard refer to (Ghaffaripour et al., 2017).

Using a novel three-point time marching approach with second order accuracy (Khoshghalb et al., 2011), equations (4) and (5) are discretised in time as follows:

$$A\mathbf{K}\mathbf{U}^{t+\alpha\Delta t}+A\mathbf{Q}\mathbf{P}^{t+\alpha\Delta t}=A\mathbf{F}_{\mathrm{s}}^{t+\alpha\Delta t} \tag{6}$$

$$\begin{aligned}&A\mathbf{Q}^{\mathrm{T}}\mathbf{U}^{t+\alpha\Delta t}-\left(\Delta t\mathbf{H}+A\mathbf{M}\right)\mathbf{P}^{t+\alpha\Delta t}=\Delta t\mathbf{F}_{\mathrm{w}}^{t+\alpha\Delta t}+\\&B\mathbf{Q}^{\mathrm{T}}\mathbf{U}^{t}-C\mathbf{Q}^{\mathrm{T}}\mathbf{U}^{t-\Delta t}-Ba_{\mathrm{w}}\mathbf{M}\mathbf{P}^{t}+Ca_{\mathrm{w}}\mathbf{M}\mathbf{P}^{t-\Delta t}\end{aligned} \tag{7}$$

where α is the growth factor in the time discretisation scheme.

5 ORDER OF ACCURACY STUDY

The order of accuracy study is a rigorous code verification test, which examines whether or not the discretisation error of the numerical solution is reduced at the expected rate (Roy, 2005). In the order of accuracy test, the order of accuracy for the numerical scheme is obtained as the mesh and the time step are systematically refined by evaluating the reduction rate of various norms of the solution discretisation error over the domain. The error norms that are often used are L_2 and L_∞. For any state variable w (u_1, u_2 or p), these error norms are defined in this study as follows,

$$L_\infty=\left\|\mathbf{w}^{\mathrm{a}}-\mathbf{w}^{\mathrm{n}}\right\|=\max_{i=1}^{n'_{\mathrm{n}}}\left|w_i^{\mathrm{a}}-w_i^{\mathrm{n}}\right| \tag{8}$$

$$L_2=\sqrt{\frac{1}{n'_{\mathrm{n}}}\sum_{i=1}^{n'_{\mathrm{n}}}\left(w_i^{\mathrm{a}}-w_i^{\mathrm{n}}\right)^2} \tag{9}$$

where L_∞ is the infinity norm and L_2 is the second norm. $\mathbf{w}^{\mathrm{a}}$ and $\mathbf{w}^{\mathrm{n}}$ are the analytical and numerical solution vectors for the state variable of interest, respectively, where w_i^{a} and w_i^{n} are the entries of these vectors for each node of interest. The variable n'_{n} is the total number of field nodes on which no essential boundary condition is applied.

5.1 *Numerical order of accuracy*

Oberkampf and Roy (2010) proposed an approach to obtain the spatial order of accuracy in transient problems. To this end, neglecting the higher order terms, the discretisation error of the equations presented at ith spatial discretisation and jth temporal discretisation can be written in the following form

$$E_{ij}^{L}=\beta_{\mathrm{h}}h_i^{r_{\mathrm{h}}}+\beta_{\mathrm{t}}\tau_j^{r_{\mathrm{t}}}+O\left(h_i^{r_{\mathrm{h}}+1}\right)+O\left(\tau_j^{r_{\mathrm{t}}+1}\right) \tag{10}$$

where r_h and r_τ are the orders of accuracy in space and time, respectively, β_h and β_t are the coefficients of spatial and temporal terms, respectively, h_i and τ_j are normalized spatial and temporal discretisation sizes corresponding to the ith spatial discretisation and jth temporal discretisation, respectively, and L is the error norm used for order of accuracy study ($L = L_2$ or L_∞). The higher order terms, $O\left(h_i^{r_h+1}\right)$ and $O\left(\tau_j^{r_\tau+1}\right)$, can be neglected if the spatial and temporal discretisations adopted are in the asymptotic convergence range. The asymptotic range is defined as the range of discretisation sizes where the lowest-order terms in the truncation error dominate. For the developments to follow, it is assumed that the solution is in asymptotic range; however, it is noted that the identification of the asymptotic range may be challenging for complex scientific computing applications (Oberkampf and Roy, 2010).

To obtain the spatial order of accuracy of the code, a constant time step is selected ($j = \mathrm{c}$) rendering the temporal discretisation error term in equation (10) a constant. Spatial discretisation errors are then found through systematic mesh refinements. Neglecting the higher order terms, for three spatial discretisations ($i = 1$ to $i = 3$), we have

$$E_{i\mathrm{c}}^L = \beta_h h_i^{r_h} + \beta_t \tau_c^{r_\tau} \tag{11}$$

Exploiting the constancy of the temporal discretisation error term, we then have

$$E_{i\mathrm{c}}^L - E_{(i-1)\mathrm{c}}^L = \beta_h \left(h_i^{r_h} - h_{i-1}^{r_h}\right) \tag{12}$$

If the exact solution is known, the errors can be evaluated for each numerical solution. Thus, we have

$$\frac{E_{1\mathrm{c}}^L - E_{2\mathrm{c}}^L}{E_{2\mathrm{c}}^L - E_{3\mathrm{c}}^L} = \frac{h_1^{r_h} - h_2^{r_h}}{h_2^{r_h} - h_3^{r_h}} = \frac{\left(h_1/h_2\right)^{r_h} - 1}{1 - \left(h_3/h_2\right)^{r_h}} \tag{13}$$

Now, introducing the spatial discretisation refinement factor $R = h_2/h_1 = h_3/h_2$ (i.e., the ratio between element sizes of two consecutive meshes in the mesh refinement study), the observed order of accuracy for spatial discretisation, r_h, can be obtained from equation (14) as follows

$$r_h = \frac{1}{\ln R} \ln\left(\frac{E_{2\mathrm{c}}^L - E_{3c}^L}{E_{1\mathrm{c}}^L - E_{2\mathrm{c}}^L}\right) \tag{15}$$

This numerical order of accuracy is then compared with the formal order of accuracy, obtained or estimated from a truncation error analysis of the discrete equations or interpolation theory, depending on the numerical solution scheme adopted (Roy, 2005; Choudhary et al., 2016). If the discretisation error of the numerical solution does not reduce monotonically, or if the order of accuracy obtained from the numerical solutions fails to match the formal order of accuracy, these could be indications of a probable coding mistake or algorithm inconsistency.

As can be seen, the exact solution to the governing equations, which is often unavailable, is required in this procedure. A method to address this difficulty is discussed later in this paper. It is also worth noting that the temporal order of accuracy can be obtained in a similar fashion based on several analyses using same spatial discretisations, but different temporal discretisations. The temporal order of accuracy is not discussed in this study due to the length limitations.

It is worth mentioning that there is no iterative procedure involved in the problems studied in this chapter. It is also assumed that the round-off error is negligible compared to the overall discretisation error of the solutions

5.2 *Formal order of accuracy*

The formal order of accuracy is the theoretical rate of convergence of the discrete solution to the exact solution to the mathematical model. For simple mathematical models and simple solution/discretisation methods, this can be obtained using truncation error analysis of the discrete equations or interpolation theory. For example, when finite difference method (FDM) is used for the solution of a parabolic equation, the formal spatial order of accuracy can be obtained using a truncation error analysis (e.g., (Roy, 2005)).

In this study, the ESPIM along with a three point time discretisation technique is applied to coupled flow and deformation problems in two phase saturated porous media. Due to the complexity of the governing equations and the numerical solution technique adopted in this study, determination of the spatial formal order of accuracy directly from the governing equations is difficult, if not impossible. Hence, another approach, called the residual method, is adopted for estimation of the spatial formal order of accuracy. In this approach, the exact solution to the mathematical model is substituted into the discrete governing equations. The exact solution to the mathematical model does not satisfy the discrete equations, and it can be shown that for linear problems, the remainder (referred to as discrete residual) approximates the spatial truncation error (Oberkampf and Roy, 2010). Therefore, by performing a systematic mesh refinement (with a constant time discretisation), and evaluating the discrete residual in each case, the reduction rate of the spatial truncation error can be estimated, which is the spatial formal order of accuracy of the numerical scheme.

5.3 *Method of manufactured solutions*

As explained earlier, exact solutions to the governing equations are required in an order of accuracy study to obtain the numerical orders of accuracy.

However, except for a limited number of simple cases, exact solutions are often not available for real geotechnical engineering problems with complex initial and boundary conditions. Even when exact solutions are found for such complex problems, they are often resulted from significant simplifications assumed in the problems.

Due to the unavailability of the exact solutions in most cases, the method of manufactured solutions (MMS) can be utilised as an alternative approach to provide a straightforward and general procedure for generating analytical solution of complex system of PDEs for code verifications. As far as the adopted manufactured solutions (MSs) are not mathematically problematic, their physical meaning is of no importance in conducting an order of accuracy test (Roy, 2005).

The basic idea behind the MMS is to manufacture exact continuum solutions to the PDEs of interest (Roache, 2002). To this end, analytic solution to the PDEs are first assumed and next, the selected MS is substituted into the PDEs to calculate the source terms which guarantee that the selected MSs are indeed exact solutions to the governing PDEs. The source terms are distributed terms which should be applied in the code at each node of interest, according to the nature of the ESPIM code in hand. The source code must, therefore, be accessible and open to modifications so that such an implementation can be made when using the MMS. The MMS may therefore not be applicable to commercial codes, unless the source code can be accessed.

6 NUMERICAL EXAMPLE

A $2\text{m}\times 2\text{m}$ weightless isotropic saturated porous medium is considered in a plain strain setting, in which $-1\,\text{m}\le x\le 1\,\text{m}$ and $0\le y\le 2\,\text{m}$. The state variables u_1, u_2 and p are assumed known on the domain boundaries where the essential boundary conditions are imposed. Linear elasticity is assumed for the mechanical behaviour of the solid phase. The material parameters adopted in the numerical analyses are given in Table 1.

Table 1. Material properties for the numerical analyses.

Parameter	Value
Young's modulus (E)	10,000 kPa
Poisson's ratio (v)	0.3
Porosity (n)	0.5
Intrinsic permeability (k)	10^{-10} m^2
Water density (ρ_w)	1.0 t/m^3
Water dynamic viscosity (μ_w)	10^{-6} kPa.s
Compressibility of fluid (c_w)	4.54×10^{-7} kPa^{-1}

A time step increment of $\Delta t = 0.1\,\text{s}$ and a time step growth factor of $\alpha = 1.0$ are assumed for the numerical analyses to obtain spatial order of convergence. Five different models using different background meshes are used for evaluating the solution errors at a nominal time of $\text{t} = 10\text{s}$, which are detailed in Table 2. The background mesh sizes in Table 2 are obtained from $h = \sqrt{\Omega}/\left(\sqrt{n_\text{n}}-1\right)$ (Liu and Zhang, 2013), where Ω is the area of the domain and n_n is the total number of nodes.

Table 2. The properties of different mesh configurations for the numerical examples.

Mesh number	Number of nodes	Number of cells	Mesh size (m)
1	41	64	0.370
2	145	256	0.181
3	545	1024	0.090
4	2113	4096	0.044
5	8321	16384	0.022

Now, a solution with a "proper" analytical functions must be "manufactured" for this problem. The MS does not necessarily need to be physically realistic and can involve general analytical functions. The following set of MSs are selected according to the general recommendation by Oberkampf and Roy (2010),

$$u_1 = 0.02 + 0.01(x^2-1)^2(y^2-2y)^2\cos(\frac{\pi t}{9}) \times\left(3\sin(\frac{5\pi x}{4}) - 2\sin(\frac{3\pi y}{4}) + \cos(\pi xy)\right) \tag{16}$$

$$u_2 = -0.01 + 0.01(x^2-1)^2(y^2-2y)^2\sin(\frac{\pi t}{15}) \times\left(\sin(\frac{3\pi x}{4}) + 2\cos(\pi y) - \sin(\frac{5\pi xy}{4})\right) \tag{17}$$

$$p = 200 + 5(x^2-1)^2(y^2-2y)^2\cos(\frac{\pi t}{12}) \times\left(3\sin(\pi x) - \cos(\frac{5\pi xy}{4}) - \cos(\frac{3\pi xy}{4})\right) \tag{18}$$

Following recommendations by Bond et al. (2007), the sinusoidal parts of the MSs are multiplied by $(x^2-1)^2(y^2-2y)^2$ to ensure that the boundary conditions for the MSs are simple, similar to the boundary conditions relevant in real applications of the code. A trigonometric function of time is also multiplied to the MSs to induce time dependency of the solution.

The variations of the discretisation error norms of the numerical solutions are depicted in a logarithmic scale in Figure 1 as a function of the mesh size for this example. Presented in Figure 2 are the observed (or numerical) orders of accuracy for the three state variables using L_2 and L_∞ norms of the discretisation error, obtained from equation (19). It is observed that the orders of accuracy are close to 2, especially when finer discretisations are used.

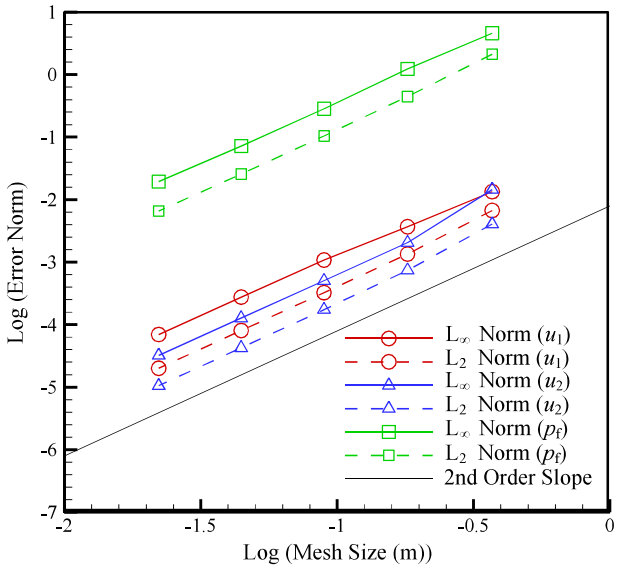

Figure 1. Mesh convergence study at t=10 s for obtaining the observed spatial orders of accuracy.

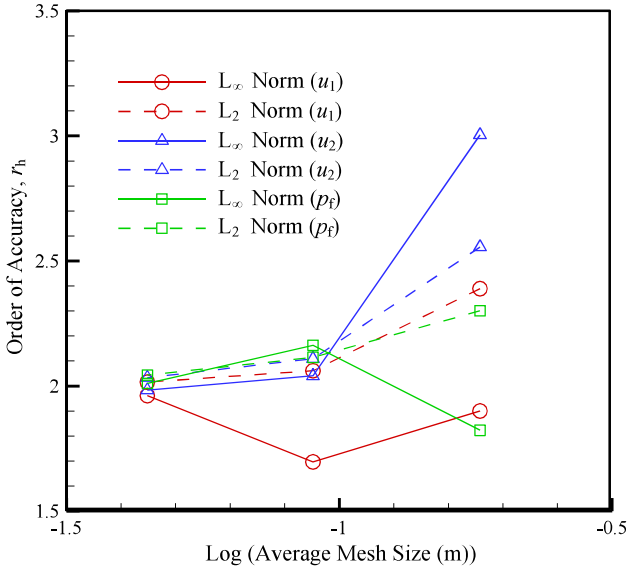

Figure 2. Observed spatial orders of accuracy at t=10 s

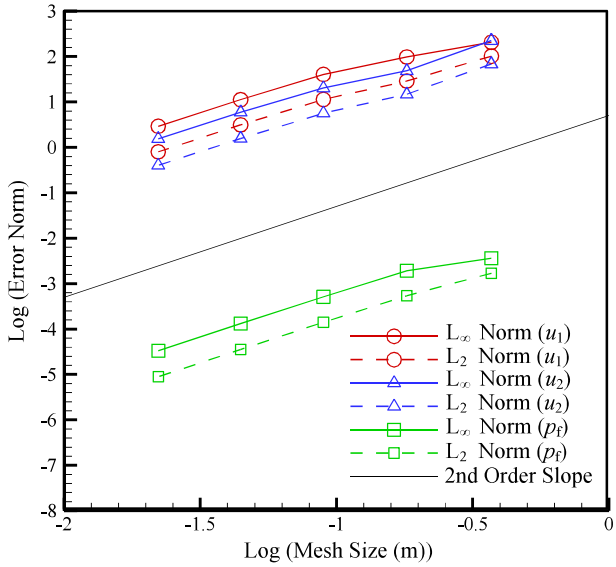

Figure 3. Order of accuracy study at t=10 s for obtaining the formal spatial orders of accuracy.

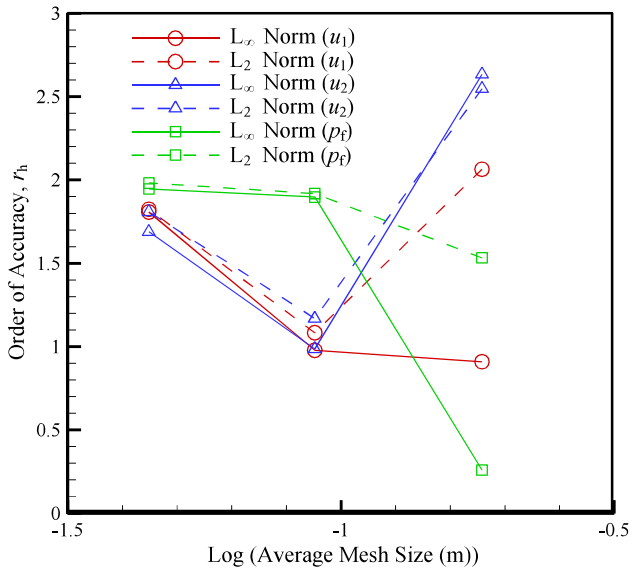

Figure 4. Formal spatial orders of accuracy at t=10 s

The formal orders of accuracy for the state variables, obtained using the procedure explained earlier in section 5.2, are illustrated in Figures 3 and 4. It is observed that the formal orders of accuracy approach 2.0 for both L_2 and L_∞ norms as the element size reduces, which is in excellent agreement with the numerically observed convergence rates. The formal orders of accuracy, however, slightly deviates from 2 as coarser discretisations are used. This problem is due to inability of coarse background meshes in accurate prediction of the complicated MSs adopted in equations (16) to (18).

In linear analyses, the study of the accuracy and convergence of the numerical solution are often performed in terms of the energy error norm, E_e, defined as,

$$E_e = \frac{1}{\Omega}\sqrt{\frac{1}{2}\sum_{k=1}^{n_{\mathrm{SD}}}\int_{\Omega_k^{\mathrm{SD}}}\left(\boldsymbol{\varepsilon}_k^{\mathrm{a}}-\boldsymbol{\varepsilon}_k^{\mathrm{n}}\right)^{\mathrm{T}}\mathbf{D}^{\mathrm{e}}\left(\boldsymbol{\varepsilon}_k^{\mathrm{a}}-\boldsymbol{\varepsilon}_k^{\mathrm{n}}\right)\mathrm{d}\Omega_k^{\mathrm{SD}}} \qquad (20)$$

where $\boldsymbol{\varepsilon}_k^{\mathrm{a}}$ and $\boldsymbol{\varepsilon}_k^{\mathrm{n}}$ are the analytical and numerical strain vectors corresponding to the kth smoothing domain. Figure 5 shows the numerically observed spatial convergence rate of the energy norm for different nodal discretisations at $t = 10$ s.

It is known that for smooth solutions like the adopted manufactured solution in this example, the order of accuracy for strain energy is one order lower than that of the displacements (Belytschko et al., 2000). Noting Figure 5, it can be seen that the expected first order accuracy in strain energy is also recovered as the mesh becomes finer and the solution enters the asymptotic range.

From this example, it can be seen that the formal spatial order of accuracies are recovered by the numerical solutions, and the code is therefore verified, spatially, for the selected MS.

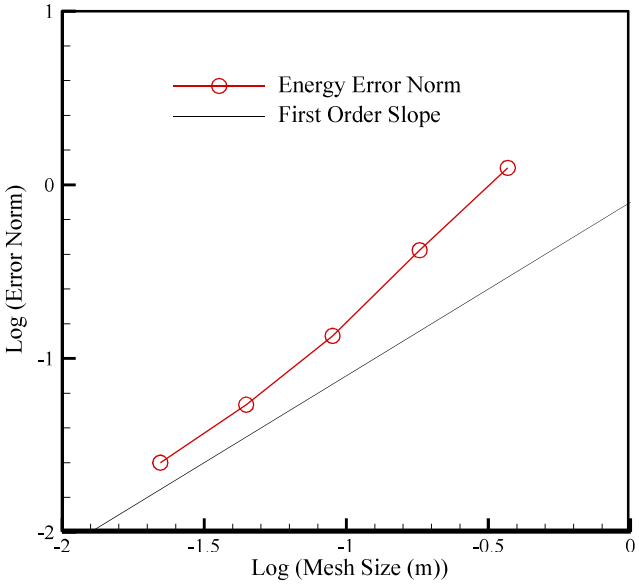

Figure 5. Energy error norm at t=10 s.

7 CONCLUSION

The application of the MMS combined with order of accuracy study for code verification in geomechanics was presented in this paper. The procedure for code verification was described in details for an ES-PIM in-house code for coupled flow and deformation analysis of poro-elastic media developed in Fortran. Verification of the code was performed through an order of accuracy study in space domain with a manufactured solution for displacement and pore pressure fields that are constructed as functions of both space and time. The results showed that the code successfully passes the spatial order of accuracy test.

REFERENCES

Belytschko, T., Liu, W. K. & Moran, B. 2000. Finite elements for nonlinear continua and structures. *J. Wiley*.

Bond, R. B., Ober, C. C., Knupp, P. M. & Bova, S. W. 2007. Manufactured solution for computational fluid dynamics boundary condition verification. *AIAA journal,* 45(9), pp 2224-2236.

Choudhary, A., Roy, C. J., Dietiker, J.-F., Shahnam, M., Garg, R. & Musser, J. 2016. Code verification for multiphase flows using the method of manufactured solutions. *International Journal of Multiphase Flow,* 80(150-163.

Ghaffaripour, O., Khoshghalb, A. & Khalili, N. 2017. An edge-based smoothed point interpolation method for elasto-plastic coupled hydro-mechanical analysis of saturated porous media. *Computers and Geotechnics,* 82(99-109.

Khoshghalb, A., Khalili, N. & Selvadurai, A. 2011. A three-point time discretization technique for parabolic partial differential equations. *International Journal for Numerical and Analytical Methods in Geomechanics,* 35(3), pp 406-418.

Lewis, R. & Schrefler, B. 1999. The finite element method in the static and dynamic deformation and consolidation of porous media. *Meccanica,* 34(3), pp 231-232.

Liu, G.-R. & Gu, Y. 2001. A point interpolation method for two-dimensional solids. *International Journal for Numerical Methods in Engineering,* 50(4), pp 937-951.

Liu, G.-R. & Zhang, G.-Y. 2013. *Smoothed point interpolation methods: G space theory and weakened weak forms*: World Scientific.

Oberkampf, W. L. & Roy, C. J. 2010. *Verification and validation in scientific computing*: Cambridge University Press.

Roache, P. J. 2002. Code verification by the method of manufactured solutions. *Journal of Fluids Engineering,* 124(1), pp 4-10.

Roy, C. J. 2005. Review of code and solution verification procedures for computational simulation. *Journal of Computational Physics,* 205(1), pp 131-156.